Some Aspects of Structures of Turbulent Pool Fires

R. S. ALGER
Stanford Research Institute
R. C. CORLETT
University of Washington
A. S. GORDON and F. A. WILLIAMS
University of California, San Diego

The results of an experimental study of the burning of JP-5 and methanol pools emphasize structural differences between JP-5 and methanol fires as well as the importance of radiant feedback of energy to the pool surface in controlling rates of burning.

LARGE POOL fires constitute a potential menace in operations involving fuel storage. Since their turbulent character is an obstacle to theoretical description and to meaningful, reproducible measurement, even rudimentary information concerning their structures can increase understanding and thereby contribute to improved procedures for fire protection. The principal previous observations consist of measurements of burning rates, flame heights, and external radiant fluxes. Blinov and Khudiakov[1,2] compiled flame heights and burning rates of common fuels as functions of pan diameter up to 3,000 cm. They established that, for diameters above about 130 cm, the fires were fully turbulent, the burning rate being independent of pan diameter. The present study concerns methanol and JP-5, burning in pans 305 cm in diameter well into the turbulent range. The objective is to gain understanding of somewhat more detailed aspects of these fires, including composition and temperature structures and radiant flux to the fuel surface, with finer resolution in space and time than that achieved in work discussed previously.[3-8]

JP-5 is a multicomponent hydrocarbon having a high heat of combustion, a large liquid burning rate, and luminous, smoky flames. In contrast, methanol is a single compound with a low heat of combustion and burning rate, having faint blue flames, visible in darkness, approaching very close to the fuel surface. The stoichiometrically required mass ratios of air to fuel are 15 for JP-5 and 6.5 for methanol. These two fuels were selected to accentuate differences in fire behavior.

EXPERIMENTAL PROCEDURE AND EQUIPMENT

For methanol fires, the steel pan was filled to a depth of about 5.1 cm with fuel. For JP-5 fires, about 2.8 cm of fuel was floated on about 2.3 cm of water. The water layer provided a level base and protected the pan from excessive temperatures during burnout. The fuel amounts were sufficient for attainment of quasisteady burning, which lasted 20 to 30 min for methanol and 5 to 10 min for JP-5. Heat transfer through the pan rim is negligible. Run-to-run variations in fuel and substrate temperatures had no apparent effect during quasisteady burning. However, these variables influenced rates of fire spread and times required to reach constant burning rate. For example, on warm days methanol (flash point 15° C) ignited quickly through the vapor above the pool, but on cold mornings flames spread as the fuel heated, the spread being accompanied by a liquid ripple.

Since flame and smoke plume geometries are sensitive to air motion, all tests were run at wind less than 200 cm s^{-1}. Nevertheless, the influence of wind often was evident. To minimize complications of extrapolating from one fire to another, a variety of parameters were measured simultaneously; Table 1 lists the techniques, and Figure 1 shows the experimental arrangement. A Gill propeller-vane anemometer, two pan diameters from the fire, measured wind velocity. Its threshold and 90 percent full responses were 15 cm s^{-1} and 52 cm s^{-1}; gust response of 90 percent occurred for 900 cm sinusoidal fluctuations. For some methanol fires, smoke generators were used to provide general patterns of inflowing air and of the plume.

Burning weight data were obtained by (1) monitoring the weight of the pan and fuel on hydraulic load cells at three points of support, (2) observing fuel levels by remote manometers, and (3) measuring hydrostatic pressure by a load cell mounted in the base of the pan. The third-mentioned approach was the most free from operational difficulties. The pressure-sensitive cell was calibrated as fuel was added to the pan. Since burning rates are obtained

TABLE 1. *Measurement Techniques*

Parameter	*Technique*
Air Velocity and Direction	Recording Anemometer
Burning Rate	Weight Loss
Flame Geometry	Time-Lapse Photography
Temperatures	Thermocouples, Coarse and Fine
Compositions:	
O_2, CO_2, CO, N_2	On-Line Gas Chromatography
These and Other Constituents	Grab Samples for Laboratory Analysis
O_2, CO_2, CO	On-Line Non-Dispersive Infrared and Beckman Conductivity Cell
Radiation Field:	
At Fuel Surface	Transpiration Radiometer and Gardon Radiometers
External	Gardon Radiometers and Thermopiles
Atmospheric Absorption	Telescopic Radiometer

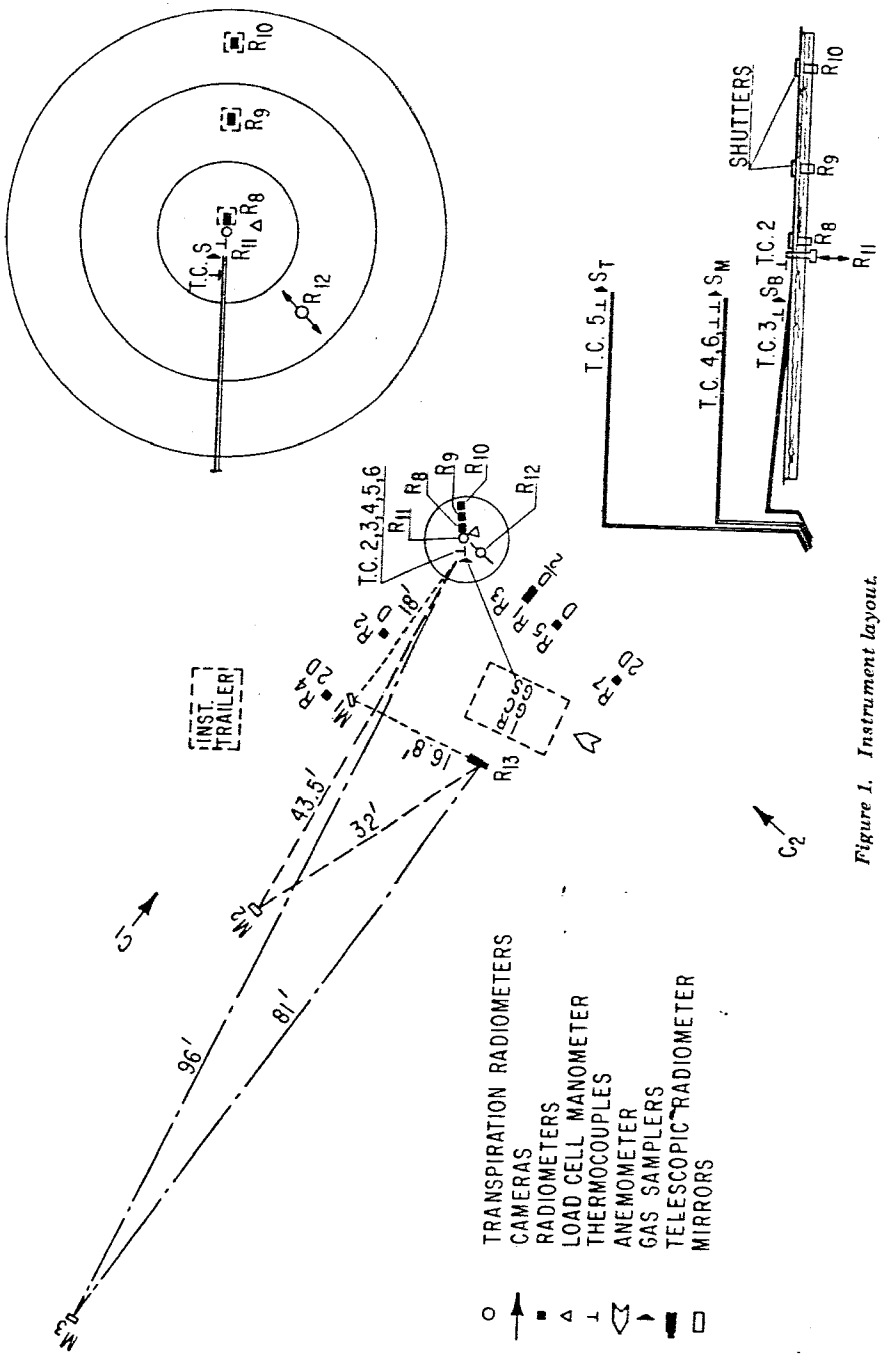

Figure 1. Instrument layout.

from the slope of the weight curve, changes in absolute pressure due to plume buoyancy or aerodynamic phenomena cancel if the effect remains reasonably constant over the measurement interval. Hence the third method is a good indicator of liquid regression rate.

Flame shapes and sizes were recorded at one-second intervals by two super-8 time-lapse cameras. Each frame was pip-marked on temperature and radiation data traces. This facilitates comparisons which show, for example, that in JP-5 fires, peaks in radiation intensity occur when bright yellow "fireballs" break through the smoke, whereas methanol fires exhibit fewer fluctuations in radiation intensity.

Temperatures were monitored near openings of the sampling probes, as indicated by T. C. 3, 4, 5, and 6 in Figure 1. All thermocouples were 250μ chromel-alumel except T. C. 6, which was 25μ Pt-Pt 10 percent Rh, selected for fast response. Some insight into turbulent characteristics of the fire is provided by signals from adjacent T. C. 4 and 6. Both traces exhibit the same general peak and valley structure, but T. C. 6 reveals a fine structure of 4 to 5 peaks per second, compared to about .5 to 1 peak per second for T. C. 4; true frequencies may be higher than that of T. C. 6. T. C. 2 was attached to the radiometer mount vertically movable in the center of the pan; in the down position the junction is submerged in fuel, and at the maximum elevation the junction is several inches above the surface.

Nondispersive infrared monitoring of carbon dioxide (CO_2) and carbon monoxide (CO), and conductivity-analyzer monitoring of oxygen (O_2) provided continuous records used to guide sample collection for more accurate analysis. Grab samples were obtained with 2-liter glass flasks, filled by periodically diverting products from continuous sampling lines that are directed into a portable gas chromatograph. Only one to four grab samples and gas chromatographic analyses could be obtained during the course of a run. Due to mixing in sampling lines, all recorded compositions represent averages. Instruments were calibrated by injecting standard gas mixtures into the sampling ports (Figure 2).

Four types of radiometers were employed:

• *Transpiration radiometers, R_{11}, and R_{12}.* These windowless instruments have a 180° field of view and avoid convective heating by passing a stream of nitrogen through the black porous detector element. In principle, both the total incident energy and the radiation component can be measured by operating the instrument without and with the nitrogen flow. R_{11} in the center of the pan was on a hydraulic piston and could be moved up and down several inches from the fuel surface. R_{12} was mounted on a long pivot, and could travel horizontally through the flames at elevations from 1 to 3 ft above the fuel surface. At the extreme outward position, R_{12} was adjacent to R_1 and R_3, thereby permitting an intercomparison with these stationary instruments. Considerable difficulty was experienced with the electrical coupling to R_{12}; however, on successful runs, the radiation levels were compatible with those observed for R_{11} (1.1 to 1.6 and 1.1 to 2.4 cal cm^{-2} s^{-1} for methanol and JP-5).

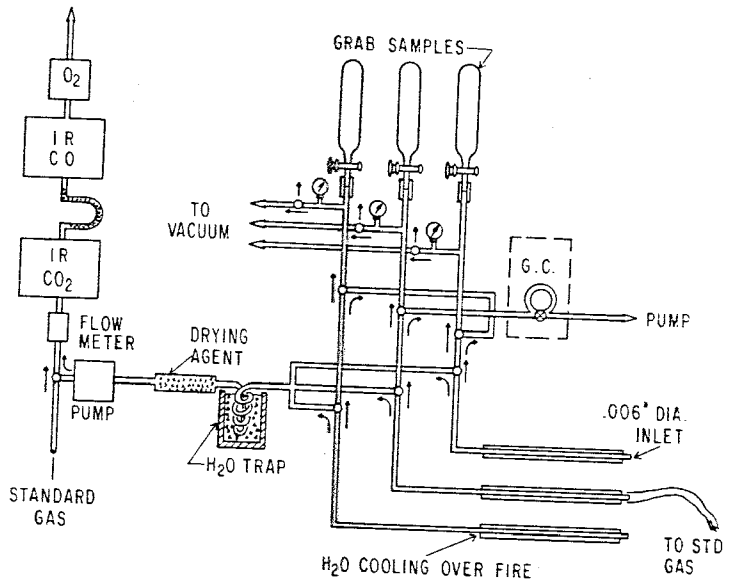

Figure 2. Gas analysis system.

• *Gardon type Hi-Cal radiometers* R_1, R_2, R_3, R_5, R_8, R_9, R_{10}. Radiometers R_8, R_9, and R_{10} measured the radiation returning to the fuel surface at three positions. These radiometers, equipped with sapphire windows and additional water cooling, commenced each burn slightly below the surface of the fuel. In the course of the fires, the fuel level receded and the radiometers emerged into the combustion zone where they were exposed to the full feedback energy. The sapphire windows were expected to heat during a fire and pass additional energy to the sensitive element; therefore, each radiometer was covered with a water-cooled shutter that opened periodically for radiation measurements, then closed to indicate the background contribution from the warm windows. Since the transmission losses in the windows were unknown for the flame spectra involved, R_8 was calibrated by comparison to R_{11}, and the same loss factor was applied to R_9 and R_{10}. Total feedback heat values were calculated by applying radiometer data uniformly to the pan areas indicated in Figure 1.

• *Thermopiles,* R_4 *and* R_7. Radiation intensities outside the combustion zone were measured with a combination of Hi-Cal radiometers at the close-in stations, i.e., R_1, R_2, R_3, R_5, and the more sensitive thermopiles R_4 and R_7 at the greatest distances. All of these instruments had windows to minimize the effects of air currents, i.e., sodium chloride (NaCl) for R_1, R_2, and R_5, sapphire for R_3, and saran for R_4 and R_7. No significant differences was observed between the sapphire and NaCl windows.

• *Telescopic Radiometer.* R_{13}, the telescopic radiometer and the three front-surfaced mirrors M_1, M_2, and M_3 were arranged as shown in Figure 1 to measure the radiant energy absorbed by the atmosphere. In large fire tests where the distance 2D corresponds to several hundred feet, atmospheric absorption presumably causes the observed radiation field to decrease with distance more rapidly than the view factor and inverse square law predict. R_{13} repeatedly examined the same area of the combustion zone along the three different path lengths obtained by sighting on the mirrors. For JP-5 flames, the absorption was less than 30 percent over the 52-m distance, but with methanol flames, this loss increased to about 60 percent.

All of the signals from load cells, thermocouples, radiometers, cameras, and the anemometers were processed and recorded in the instrument trailer (Figure 1). Where modest time resolution or an immediately available record was required, the signals were recorded on visicorders. Other signals were recorded on a twenty-channel magnetic tape system. This complexity is dictated by the requirement of obtaining various kinds of information simultaneously.

COMPOSITION AND TEMPERATURE STRUCTURE

A pronounced characteristic of the results of both composition and temperature measurements is the high level of fluctuations revealed. For example, at 1 cm above the center of a JP-5 pool, some samples showed essentially no oxygen while others showed near ambient oxygen concentrations. The fine thermocouples showed temperatures varying from ambient to 1,200° C in the methanol fires. Clearly, both fuel eddies and air eddies were present down to very low elevations, even in the center of the pool. Consistent with differences in stoichiometry, the composition measurements suggest that nearly pure-fuel eddies are more likely for JP-5 and that nearly pure-air eddies are more likely to penetrate to the center of the fire for methanol.

It is of interest to attempt to extract from composition measurements concentrations of major species that were not measured, notably water vapor and fuel. The requisite methods differ for the two fuels. The gas is composed primarily of N_2, O_2, CO_2, H_2O and fuel, denoted symbolically by F. Since N_2 was present in all samples, it serves as a useful reference species. Let r_i denote the ratio of molar concentration of species i to that of N_2. Then the carbon-hydrogen and oxygen-nitrogen ratios may be written as

$$C/H = (r_{CO_2} + r_{CO} + nr_F)/(2r_{H_2O} + mr_F) \quad (1)$$

and

$$O/N = r_{O_2} + r_{CO_2} + r_{CO}/2 + r_{H_2O}/2 + l\,r_F/2, \quad (2)$$

respectively, where l, m and n denote the average number of oxygen, hydrogen and carbon atoms, respectively, in the gaseous fuel species, per

molecule. For methanol, $l = 1, m = 4$ and $n = 1$, while for JP-5, $l = 0$ and $m \approx 9$ n/4, but the value of n is more variable. If n and r_F can be found, then the fuel-oxygen molar equivalence ratio can be calculated from the carbon-based formula

$$\varphi = 3.72\,(r_{CO_2} + r_{CO} + n r_F), \tag{3}$$

derived by observing that, since the stoichiometric carbon atom-oxygen molecule ratio is unity, the stoichiometric carbon atom-nitrogen molecule ratio is the air value, 1/3.72, of the oxygen-nitrogen ratio.

For JP-5, the absence of oxygen in the fuel implies that O/N = 1/3.72; therefore, Equation 2 gives r_{H_2O} directly. In Equation 1, C/H will be known only if relative diffusion of C-containing and H-containing species is neglected, and under these conditions Equation 1 reduces to

$$r_{H_2O} = (r_{CO_2} + r_{CO})/(2C/H). \tag{4}$$

Although Equation 4 provides an alternative method for calculating r_{H_2O} and therefore offers a check on the result obtained from Equation 1, it does not enable the relative concentration of fuel to be obtained. Therefore, for JP-5, equivalence ratios can be calculated from the data only in regions where fuel concentrations are negligible in comparison with those of CO_2 and CO. In other regions, use of Equation 3 with $r_F = 0$ provides only a lower bound for φ.

For methanol, the oxygen in the fuel prevents r_{H_2O} from being obtained directly from Equation 2. However, neglect of relative diffusion still permits this quantity to be calculated from Equation 4. By putting $O = O_{fuel} + O_{air}$ and $N = 3.72\ O_{air}$ in Equation 1, use may be made of Equation 3 along with the alternative expression $\varphi = (O_{fuel}/O_{air})/(O_{fuel}/O_{air})_{stoichiometric}$, in which the denominator equals 1/3, to obtain by equating two alternative expressions for φ the formula

$$r_F = (6 - 6\,r_{O_2} - 10\,r_{CO_2} - 7\,r_{CO})/3.72\,. \tag{5}$$

Equation 5 enables the fuel-nitrogen ratio to be obtained for methanol from available data, and Equation 3 can then be used to calculate the equivalence ratio. The presence of oxygen in the fuel molecule removes the cross check on the water vapor calculation but enables more complete composition information to be calculated.

Figure 3 shows vertical mean composition profiles, with H_2O and φ information extracted as described above. These profiles conform qualitatively to expectation. The average oxygen concentration increases with height, while that of product species decreases. Most data were taken at the 1-cm elevation because the largest number of compounds was observed there. The high variability in the average concentrations at the 1-cm height for methanol may be seen in Figure 3 and also in the sample data given in Table 2. Especially highly variable, compared with other measured species, was the CO concentration. This produces a large variation in the calculated H_2O concentration, the level of which is large, as expected in methanol fires.

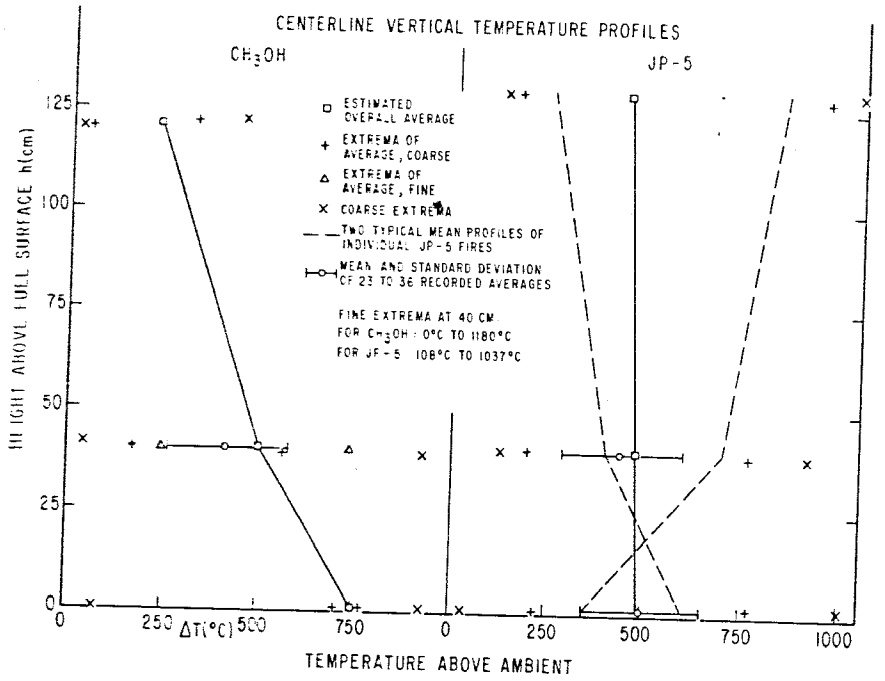

Figure 3. Centerline vertical composition profiles.

Calculated concentrations of fuel species nearly always were very small. It may be observed that, even at 1 cm, the average calculated φ is well below unity, there being only one sample having a value in excess of unity. It may be inferred that turbulent oxygen transport is efficient in methanol fires, that most fuel species burn within 1 cm of the liquid surface, and that the faint blue luminosity above 1 cm arises almost entirely from combustion of CO, which is known to occur more slowly.

For JP-5, insufficient composition data were obtained to plot profiles. It was found that r_{H_2O}, calculated by two different methods, agreed well for intermediate values of r_{CO_2} and r_{CO}. When fuel and product concentrations are low, there are large inaccuracies in the calculation from Equation 1; and when fuel concentrations are high, there are inaccuracies in use of Equation 4. In general, at the 1-cm elevation, O_2 fractions from 0 to at least 0.15, CO_2 from 0.001 to at least 0.08, CO from 0 to at least 0.06, H_2O from 0 to at least 0.15, and fuels up to at least 0.30 are found. Equivalence ratios, estimated from data of the type in Table 2, vary widely, covering values below and above unity at the 1-cm height. Substantial fuel pyrolysis is evident in the third entry of Table 2. At the 120-cm elevation, data for which are typified by the final entry in Table 2, average oxygen concentrations are higher; yet CO_2 and CO fractions reach at least 0.03 and 0.01, respectively, while equivalence ratios from 0 to at least 0.25 occur. Clearly measured concentra-

TABLE 2. *Representative Data on Relative Compositions Obtained from Grab Samples*

Fuel	*Height*	N_2	O_2	CO_2	CO	H_2	CH_4	C_2H_4	C_2H_6	C_3H_6	C_4H_8
CH_3OH	1 cm	86.25	10.1	3.0	0.5	0.19	—				
CH_3OH	1 cm	77.4	10.64	4.2	5.01	2.42	0.29				
JP-5	1 cm	52.8	0.02	5.5	6.9	4.5	11.6	9.0	1.5	4.5	3.7
JP-5	1 cm	85.9	11.22		1.62	0.44	0.7				
JP-5	120 cm	76.0	9.16	3.55	1.67	0.62	0.72	0.9			

tions of fuel-containing species decreases much less rapidly with height for JP-5 than for methanol.

Figure 4 shows vertical mean-temperature profiles, not only averages and standard deviations, but also maxima and minima of averages as well as maxima and minima of individual thermocouple readings. For methanol, the average temperature at the 1-cm elevation exhibits little scatter, although large fluctuations of high frequency occur. For JP-5 there are larger fluctuations at this height and also appreciable run-to-run deviations in the mean. For methanol at 40 cm, high-frequency and run-to-run variations are appreciable, but the average temperature definitely decreases. For JP-5, on the other hand, at 40 cm there is little or no change in the mean. At 120 cm, both the mean value and the magnitude of fluctuation decrease substantially for methanol but change little for JP-5. This is consistent with differences in measured compositions and suggest that burning is nearly completed at the highest elevation for methanol but not for JP-5, since penetration of pure air to the center occurs more readily for methanol. The dashed lines in Figure 4 show that it is possible to have significant run-to-run differences in mean vertical profiles of temperature for JP-5 fires. Occurrence of different mean profiles for the same fuel is likely to be caused at least partially by uncontrolled experimental conditions, notably wind.

In general, the main observation to be drawn from these profiles is that the heat release occurs relatively high above the fire for the hydrocarbon and extremely close to the surface for the alcohol. The relatively large heat of vaporization and the relatively low heat of combustion for the alcohol may contribute to this difference. In addition, the stoichiometry for the alcohol favors locating the flame closer to the fuel surface. The extent to which these differences influence the structure of the fire is remarkable. In the JP-5 fire, the upwardly billowing, soot-filled, and burning eddies bear no resemblance to the short, horizontally moving, transparent whirls with vertical axes seen dimpling the liquid surface of the methanol.

ENERGY FEEDBACK

Energy feedback can be inferred, approximately, from pool mass loss rate measurements. For each burn, a reasonably constant maximum burning mass flux $\dot{m}_{max}$ was observed for most of the run duration. This

represents a quasi-steady condition for which an energy balance, giving the inferred mean energy feedback flux $\bar{q}_{fb}$, is

$$\bar{q}_{fb} = l_{eff}\,\dot{m}_{max}\,, \qquad (6)$$

where l_{eff} is the effective latent heat, the enthalpy change from liquid at ambient temperature to vapor at pool-surface temperature. In the absence of surface temperature measurement, 20° C less than boiling point is assumed for calculating l_{eff}. For JP-5, handbook[9] thermal data (boiling point, 215° C; latent heat at 195° C, 67 cal gm^{-1}; mean specific heat, 0.54 cal gm^{-1}° C) yield l_{eff} = 167 cal gm^{-1}. For methanol, l_{eff} = 288 cal gm^{-1}. The uncertainties introduced by guessing the mean surface temperature are not large, perhaps 10 cal gm^{-1} for JP-5 and 5 cal gm^{-1} for methanol.

The above-stated energy balance neglects losses. Side losses are neglected in view of the small ratio of exposed side area to pool area ($\approx$ 0.03). Since neither fuel transmits significant thermal radiation through characteristic pool depths (as discussed subsequently), only convective bottom losses need consideration. For the JP-5 fires, measured heating of the underlying water layer, while appreciable over the course of a burn, is not a significant loss. For methanol fires, hydrodynamic instability due to back-absorption[10] of water vapor from reaction products provides a mechanism for liquid convection whose magnitude may be estimated as follows:

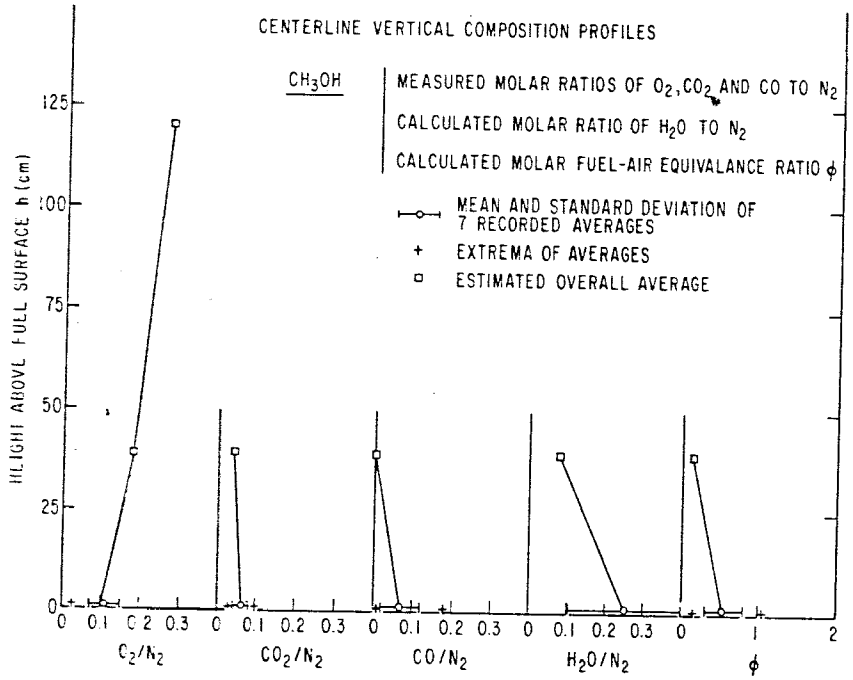

Figure 4. Centerline vertical temperature profiles.

TABLE 2. *Representative Data on Relative Compositions Obtained from Grab Samples*

Fuel	*Height*	N_2	O_2	CO_2	CO	H_2	CH_4	C_2H_4	C_2H_6	C_3H_6	C_4H_8
CH_3OH	1 cm	86.25	10.1	3.0	0.5	0.19	—				
CH_3OH	1 cm	77.4	10.64	4.2	5.01	2.42	0.29				
JP-5	1 cm	52.8	0.02	5.5	6.9	4.5	11.6	9.0	1.5	4.5	3.7
JP-5	1 cm	85.9	11.22		1.62	0.44	0.7				
JP-5	120 cm	76.0	9.16	3.55	1.67	0.62	0.72	0.9			

tions of fuel-containing species decreases much less rapidly with height for JP-5 than for methanol.

Figure 4 shows vertical mean-temperature profiles, not only averages and standard deviations, but also maxima and minima of averages as well as maxima and minima of individual thermocouple readings. For methanol, the average temperature at the 1-cm elevation exhibits little scatter, although large fluctuations of high frequency occur. For JP-5 there are larger fluctuations at this height and also appreciable run-to-run deviations in the mean. For methanol at 40 cm, high-frequency and run-to-run variations are appreciable, but the average temperature definitely decreases. For JP-5, on the other hand, at 40 cm there is little or no change in the mean. At 120 cm, both the mean value and the magnitude of fluctuation decrease substantially for methanol but change little for JP-5. This is consistent with differences in measured compositions and suggest that burning is nearly completed at the highest elevation for methanol but not for JP-5, since penetration of pure air to the center occurs more readily for methanol. The dashed lines in Figure 4 show that it is possible to have significant run-to-run differences in mean vertical profiles of temperature for JP-5 fires. Occurrence of different mean profiles for the same fuel is likely to be caused at least partially by uncontrolled experimental conditions, notably wind.

In general, the main observation to be drawn from these profiles is that the heat release occurs relatively high above the fire for the hydrocarbon and extremely close to the surface for the alcohol. The relatively large heat of vaporization and the relatively low heat of combustion for the alcohol may contribute to this difference. In addition, the stoichiometry for the alcohol favors locating the flame closer to the fuel surface. The extent to which these differences influence the structure of the fire is remarkable. In the JP-5 fire, the upwardly billowing, soot-filled, and burning eddies bear no resemblance to the short, horizontally moving, transparent whirls with vertical axes seen dimpling the liquid surface of the methanol.

ENERGY FEEDBACK

Energy feedback can be inferred, approximately, from pool mass loss rate measurements. For each burn, a reasonably constant maximum burning mass flux $\dot{m}_{max}$ was observed for most of the run duration. This

represents a quasi-steady condition for which an energy balance, giving the inferred mean energy feedback flux $\bar{q}_{fb}$, is

$$\bar{q}_{fb} \doteq l_{eff}\, \dot{m}_{max}\,, \tag{6}$$

where l_{eff} is the effective latent heat, the enthalpy change from liquid at ambient temperature to vapor at pool-surface temperature. In the absence of surface temperature measurement, 20° C less than boiling point is assumed for calculating l_{eff}. For JP-5, handbook[9] thermal data (boiling point, 215° C; latent heat at 195° C, 67 cal gm^{-1}; mean specific heat, 0.54 cal gm^{-1}° C) yield l_{eff} = 167 cal gm^{-1}. For methanol, l_{eff} = 288 cal gm^{-1}. The uncertainties introduced by guessing the mean surface temperature are not large, perhaps 10 cal gm^{-1} for JP-5 and 5 cal gm^{-1} for methanol.

The above-stated energy balance neglects losses. Side losses are neglected in view of the small ratio of exposed side area to pool area (≈ 0.03). Since neither fuel transmits significant thermal radiation through characteristic pool depths (as discussed subsequently), only convective bottom losses need consideration. For the JP-5 fires, measured heating of the underlying water layer, while appreciable over the course of a burn, is not a significant loss. For methanol fires, hydrodynamic instability due to back-absorption[10] of water vapor from reaction products provides a mechanism for liquid convection whose magnitude may be estimated as follows:

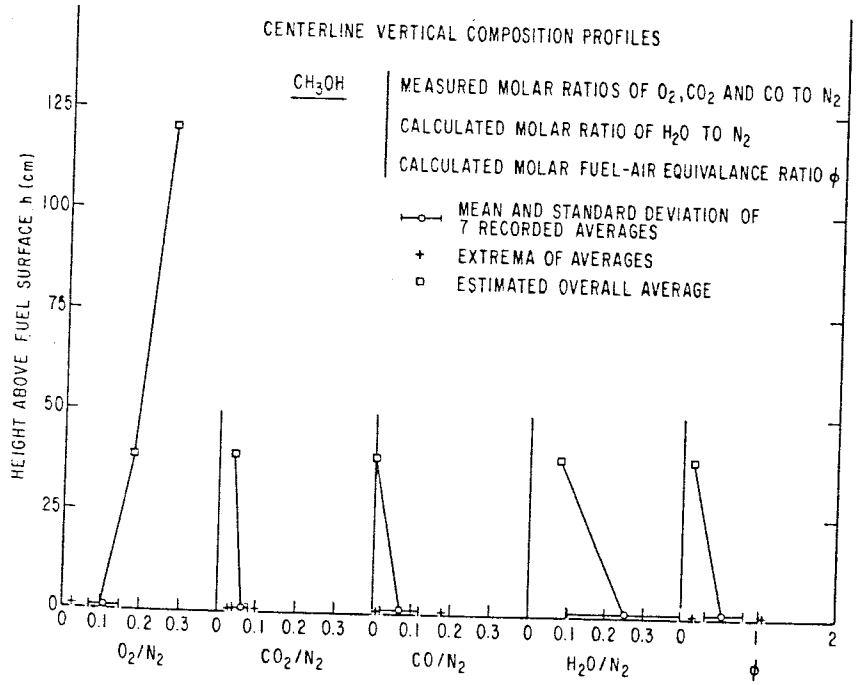

Figure 4. Centerline vertical temperature profiles.

TABLE 2. *Representative Data on Relative Compositions Obtained from Grab Samples*

Fuel	*Height*	N_2	O_2	CO_2	CO	H_2	CH_4	C_2H_4	C_2H_6	C_3H_6	C_4H_8
CH_3OH	1 cm	86.25	10.1	3.0	0.5	0.19	—				
CH_3OH	1 cm	77.4	10.64	4.2	5.01	2.42	0.29				
JP-5	1 cm	52.8	0.02	5.5	6.9	4.5	11.6	9.0	1.5	4.5	3.7
JP-5	1 cm	85.9	11.22		1.62	0.44	0.7				
JP-5	120 cm	76.0	9.16	3.55	1.67	0.62	0.72	0.9			

tions of fuel-containing species decreases much less rapidly with height for JP-5 than for methanol.

Figure 4 shows vertical mean-temperature profiles, not only averages and standard deviations, but also maxima and minima of averages as well as maxima and minima of individual thermocouple readings. For methanol, the average temperature at the 1-cm elevation exhibits little scatter, although large fluctuations of high frequency occur. For JP-5 there are larger fluctuations at this height and also appreciable run-to-run deviations in the mean. For methanol at 40 cm, high-frequency and run-to-run variations are appreciable, but the average temperature definitely decreases. For JP-5, on the other hand, at 40 cm there is little or no change in the mean. At 120 cm, both the mean value and the magnitude of fluctuation decrease substantially for methanol but change little for JP-5. This is consistent with differences in measured compositions and suggest that burning is nearly completed at the highest elevation for methanol but not for JP-5, since penetration of pure air to the center occurs more readily for methanol. The dashed lines in Figure 4 show that it is possible to have significant run-to-run differences in mean vertical profiles of temperature for JP-5 fires. Occurrence of different mean profiles for the same fuel is likely to be caused at least partially by uncontrolled experimental conditions, notably wind.

In general, the main observation to be drawn from these profiles is that the heat release occurs relatively high above the fire for the hydrocarbon and extremely close to the surface for the alcohol. The relatively large heat of vaporization and the relatively low heat of combustion for the alcohol may contribute to this difference. In addition, the stoichiometry for the alcohol favors locating the flame closer to the fuel surface. The extent to which these differences influence the structure of the fire is remarkable. In the JP-5 fire, the upwardly billowing, soot-filled, and burning eddies bear no resemblance to the short, horizontally moving, transparent whirls with vertical axes seen dimpling the liquid surface of the methanol.

ENERGY FEEDBACK

Energy feedback can be inferred, approximately, from pool mass loss rate measurements. For each burn, a reasonably constant maximum burning mass flux $\dot{m}_{max}$ was observed for most of the run duration. This

represents a quasi-steady condition for which an energy balance, giving the inferred mean energy feedback flux $\bar{q}_{fb}$, is

$$\bar{q}_{fb} = l_{eff}\,\dot{m}_{max}, \tag{6}$$

where l_{eff} is the effective latent heat, the enthalpy change from liquid at ambient temperature to vapor at pool-surface temperature. In the absence of surface temperature measurement, 20° C less than boiling point is assumed for calculating l_{eff}. For JP-5, handbook[9] thermal data (boiling point, 215° C; latent heat at 195° C, 67 cal gm^{-1}; mean specific heat, 0.54 cal gm^{-1}° C) yield l_{eff} = 167 cal gm^{-1}. For methanol, l_{eff} = 288 cal gm^{-1}. The uncertainties introduced by guessing the mean surface temperature are not large, perhaps 10 cal gm^{-1} for JP-5 and 5 cal gm^{-1} for methanol.

The above-stated energy balance neglects losses. Side losses are neglected in view of the small ratio of exposed side area to pool area ($\approx$ 0.03). Since neither fuel transmits significant thermal radiation through characteristic pool depths (as discussed subsequently), only convective bottom losses need consideration. For the JP-5 fires, measured heating of the underlying water layer, while appreciable over the course of a burn, is not a significant loss. For methanol fires, hydrodynamic instability due to back-absorption[10] of water vapor from reaction products provides a mechanism for liquid convection whose magnitude may be estimated as follows:

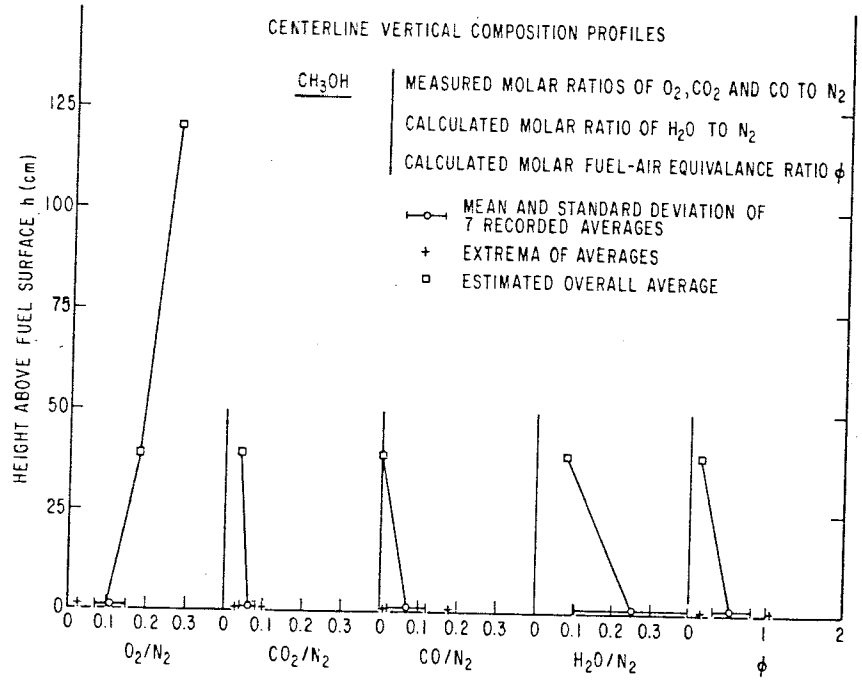

Figure 4. Centerline vertical temperature profiles.

Neglecting molecular transport, the downward fluxes of heat q_c and water $\dot{m}_w$ are proportional to respective driving forces of enthalpy $\overline{\varrho c}\ \Delta T$ and water mass concentration $\Delta\varrho_w$; i.e.

$$q_c/\dot{m}_w \approx \overline{\varrho c}\ \Delta T/\Delta\varrho_w \tag{7}$$

To estimate general magnitudes, $\dot{m}_w$ is taken[10] as 10^{-4} gm cm^{-2} s^{-1}. A lower bound for $\Delta\varrho_w$ is the methanol density differential due to thermal expansion over temperature differential ΔT, since for any lower value, the fluid layer would be stable. With this assumption, thermodynamic data for methanol yield $\Delta\varrho_w/(\overline{\varrho c}\ \Delta T) \sim 0.01$ gm cal^{-1}, so that $q_c \sim 0.01$ cal cm^{-2} s^{-1}. Although this estimate is imprecise, it is clear that downward losses are negligible.

Table 3 summarizes results for $\bar{q}_{fb}$ as given by Equation 6, together with measured values for *incident* radiative flux at pool center $q_{r,o}$ (transpiration radiometer R_{11}). In all cases, the incident center-radiation exceeds the mean feedback flux. The respective mean and variance of the ratio $\bar{q}_{fb}/q_{r,o}$ are 1.93 and 0.48 for methanol and 1.42 and 0.12 for JP-5. Thus, with high statistical confidence, for both fuels $q_{r,o} > \bar{q}_{fb}$, and with moderate confidence, the fractional excess is greater for methanol.

Of course, $q_{r,o}$ is not expected to coincide exactly with $\bar{q}_{fb}$. Undoubtedly $\bar{q}_{fb}$ contains a convective component. Also, the net heat transfer to the pool is not necessarily the same as the incident radiative flux, although such has often been assumed. Finally, the energy feedback flux $\bar{q}_{fb}$ probably varies over the pool surface.

The magnitude of convective feedback cannot be determined accurately. The uncertainty is usually made palatable by magnitude estimates indicating that radiation is the dominant feedback mode in large fires. An estimate is obtained from conventional turbulent boundary layer correlations with, for present conditions, characteristic length L ~ 150 cm (pool radius), characteristic velocity ~ 500 cm s^{-1} ($\sim\sqrt{g\ b\ L}$ with g as gravity acceleration and b as effective buoyancy ~ 2), transport properties taken as those of 500° C air, and 1,000° C driving temperature ΔT_f. The result is around 0.3 cal cm^{-2} s^{-1} and is not very sensitive to parameter guesses (except ΔT_f). In the absence of locally violent gas motions (of which there was no indication), the above boundary layer calculation should be conservatively high. Our best estimate is 0.2 cal cm^{-2} s^{-1}. Thus, convective heating is a substantial, but not dominant, fraction of the heat transfer from methanol fires. It is less significant for JP-5 fires and is of the same magnitude (or less) than the data scatter in Table 3.

TABLE 3. *Mean Energy Feedback ($\bar{q}_{fb}$) Compared with Incident Radiative Flux at Pool Center ($q_{r,o}$) Measured in cal cm^{-2} s^{-1}*

Run	*Fuel*	$\bar{q}_{fb}$	$q_{r,o}$
1	Methanol	0.81	1.52
2	Methanol	0.82	1.14
3	JP-5	0.68	—
4	JP-5	1.68	2.17
5	JP-5	1.40	—
6	JP-5	1.29	1.98
7	JP-5	1.26	1.79
8	JP-5	1.12	—
9	Methanol	0.75	1.41
10	Methanol	0.68	1.74

Some incident radiation could be reflected by or transmitted through the pools. Methanol flame radiation is heavily dominated by gas radiation of wavelength > 1 μm. JP-5 flame radiation has a black (carbon-particle) component, of which, however, only a small fraction (< 0.02) is of shorter wavelength than 1 μm for reasonable mean gas temperatures. Accurate absorption data for methanol[11] and semi-qualitative data for various hydrocarbons[12] representative of JP-5 show that negligible flame thermal radiation is transmitted through the pools of either fuel. A rough estimate (lacking detailed incident radiation spectra) yields characteristic absorption depths on the order of at least several wavelengths but much less than pool depth throughout most of the important 2 to 10 μm range.

For smooth liquid surfaces, reflectivity can be calculated from electromagnetic theory,[13] if the complex index of refraction n-ik is known. For absorption lengths substantially greater than the wavelength, the limit $k = 0$ is approximately valid. The infrared spectrum of n apparently is unavailable for either fuel. However, as n varies from 1.4 to 2, the range for organic liquids generally, the normal and hemispherical emittances vary (more or less smoothly) from 0.97 - 0.89 and 0.90 - 0.83, respectively. An accurate number for reflectivity, ϱ, requires, in addition to spectral n-data, the spectral and angular distribution of the incident radiation. Although this detailed information is absent, 0.05 - 0.10 appears to be a reasonable estimate for the reflectivity of the pools. Since negligible radiation is transmitted, the absorbed fraction of the incident radiation is 0.90 to 0.95. Similar reasoning leads to estimates of emitted radiation fluxes of 0.02 and 0.05 cal cm^{-2} s^{-1} for methanol and JP-5, respectively.

Thus the discrepancy between $\bar{q}_{fb}$ and $q_{r,o}$ in Table 3 appears to be primarily a matter of distribution. It was intended to develop distributional data with radiometers R_8, R_9 and R_{10}. For JP-5 fires, soot deposition on windows reduced transmission to an extent precluding meaningful interpretation. Even for methanol fires, uncertain window properties (noted in Section 2) preclude absolute interpretation. But the ratios of output of radiometers at various locations do provide useful information. From the radiometer locations (Figure 1), area increments in ratio 1/3/5 can be reasonably assigned to R_8, R_9 and R_{10}, respectively. From this can be estimated ratios of center/mean radiative heat transfer $q_{r,o}/\bar{q}_r$. Results for Runs 1, 2, 9 and 10 are indicted in Table 4. For Runs 1 and 2, the results are qualitatively consistent with physically-based expectations except for an apparently low reading of R_8 in Run 2. However, if a reasonable convective correction (say 0.2 cal cm^{-2} s^{-1}) is applied to $\bar{q}_{fb}$ in Table 3 to estimate $\bar{q}_r$, the resulting ratios $q_{r,o}/\bar{q}_r$ exceed 2 in conflict with Table 5, giving an unexplained discrepancy. Runs 1

and 2 were performed on a calm day, with flames apparently concentrated near the pool center. Runs 9 and 10 occurred on a breezy day with flames carried forward R_{10}, perhaps explaining the R_9/R_{10} ratio for these runs.

TABLE 4. *Radiometer-Indicated Radiation Flux Distributions for Methanol Fires*

Run	Output R_9/Output R_8	Output R_{10}/Output R_8	$q_{r,o}/\bar{q}_r$
1	0.76	0.48	1.59
2	1.22	0.81	1.09
9	0.56	0.94	1.22
10	0.52	0.94	1.24

FURTHER RADIATION CHARACTERISTICS

Radiometer output records help characterize fire unsteadiness. In general, all traces reveal oscillations on the order of 1 Hz. Although there is undoubtedly some tendency for the radiometers to cut off as frequency increases, it is judged that the dominant turbulent frequency of these fires is on the order of 1 Hz. This is consistent with the characteristic transit time (~ 1 s) of gas through fires of this size.

Figure 5 shows example traces (from R_{11}, pool center) hand-smoothed through the turbulent fluctuations. The general magnitudes of turbulent fluctuations are also indicated. For the methanol fires traced, turbulent fluctuations appear slightly larger in absolute magnitude, and the smoothed curve tends to fluctuate more rapidly. Note that fluctuations shown in this figure represent periods typical of gross fire motions (not individual eddies). For methanol fires, the fluctuations probably are due to wandering of regions of intense flaming. For JP-5 fires some wandering undoubtedly also occurs, but there are likely pulsations in addition. The data also generally exhibit gross shifts in $q_{r,o}$ on the order of 1 cal cm^{-2} s^{-1}, over longer time scales (minutes), in response to shifting wind.

Table 5 contains representative side radiation fluxes as revealed by radiometers such as R_1, R_2, R_3, R_5. For methanol, the ratios of R_1 and R_3 outputs to that of R_5 are consistent with the previous suggestion that the primary source of radiation is concentrated low over the center of the pool. For JP-5 fires, the radiation originates at significant elevations, so that effective distances to R_1 and R_3 and to R_5 are more nearly equal.

CONCLUSIONS

The results illustrate the variability of turbulent pool fires. Average properties, such as burning rates and flame heights, show similarities and have magnitudes that fall within the bands observed in other fires. However, conclusions about temporal and spatial characteristics depend on the cutoff frequency and geometrical resolutions of the sensors. There remains considerable room for improvements in equipment and techniques.

TABLE 5. *Example Exterior Radiometer Data (cal cm^{-2} s^{-1})*

Run	Fuel	t(min)	R_1	R_3	R_5	R_2	R_4	R_7
1	Methanol	4-5	0.095 (0.022)	0.088 (0.033)	0.058 (0.014)	0.052 (0.014)	0.014 (0.005)	0.014 (0.005)
2	Methanol	4-5	0.100 (0.027)	0.095 (0.027)	0.052 (0.016)	0.049 (0.008)	0.014 (0.004)	0.013 (0.003)
3	JP-5	0-1	0.34 (0.33)	0.32 (0.33)	0.24 (0.22)	0.36 (0.29)		
		2-3	0.33 (0.11)	0.33 (0.11)	0.24 (0.08)	0.43 (0.30)	0.09 (0.04)	
		4-5	0.27 (0.08)	0.76 (1.5)	0.19 (0.05)	0.57 (0.41)	0.10	
4	JP-5	0-1	0.71 (1.4)	0.76 (1.5)	0.65 (1.4)	0.14 (0.06)		

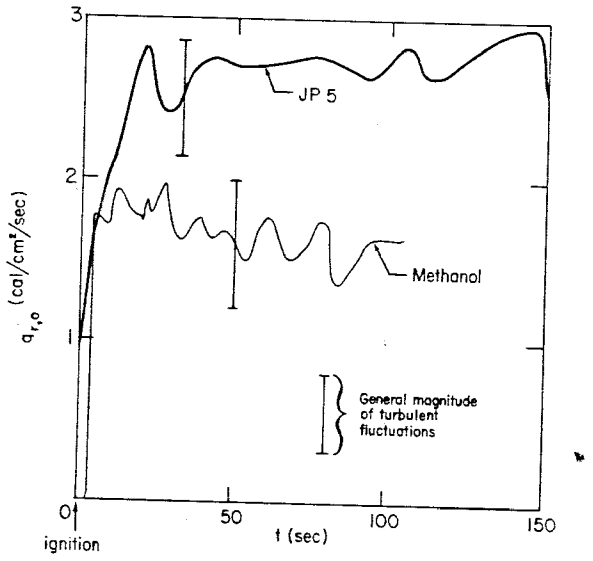

Figure 5. Example center radiation time variations (turbulent fluctuations hand-smoothed)

Structurally, the combustion zone consists of fuel eddies and air eddies that extend very close to the surface of the fuel, i.e., within a 1-cm sampling distance.

For JP-5, the combustible species extended further above the surface than for methanol. This is consistent in consideration of stoichiometry and burning rate. This difference appears to correlate with a marked difference in turbulent structure of the eddies.

Energy feedback measurements to the fuel bed require better spatial resolution before a satisfactory heat-balance can be performed. However, the present measurements confirm the dominance of radiant feedback.

The external radiation fields are in the range observed for other similar fuel fires.[14] The normalized intensities are higher than observed with larger fires because influences of atmospheric absorption increase with scale.

REFERENCES

[1] Blinov, V. I., and Khudiakov, G. N., *Doklady Akademiia Nauk SSSR*, Vol. 113 (1957), pp. 1094-1098.
[2] Hottel, H. C., *Fire Research Abstracts and Reviews*, Vol. 1 (1958), pp. 41-44.
[3] Burgess, D. S., and Grumer, J., *Fire Research Abstracts and Reviews*, Vol. 4 (1962), pp. 236-238.
[4] Spalding, D. B., *Fire Research Abstracts and Reviews*, Vol. 4 (1962), pp. 234-236.
[5] Burgess, D. S., Strasser, A., and Grumer, J., *Fire Research Abstracts and Reviews*, Vol. 3 (1961), pp. 177-192.
[6] Rasbash, D. J., Rogowski, Z. E., and Stark, G. W. V., *Fuel*, Vol. 35 (1956), pp. 94-107.
[7] Yumoto, T., *Combustion and Flame*, Vol. 17 (1971), pp. 108-110.
[8] Modak, A. T., and Croce, P.A., *Combustion and Flame*, Vol. 30 (1977), pp. 251-265.
[9] Johnson, A. J., and Auth, G. H., *Fuels and Combustion Handbook*, McGraw-Hill, New York, 1951, Chapter 5.
[10] Corlett, R. C., and Fu, T. F., *Pyrodynamics*, Vol. 4 (1966), pp. 253-269.
[11] Carlon, H. R., *Applied Optics*, Vol. 11, No. 3 (1972), pp. 549-551.
[12] "API Research Project 44 — Infrared Spectra," Carnegie Institute of Technology, Pittsburgh, 1960.
[13] Sparrow, E. M., and Cess, R. D., *Radiative Heat Transfer*, Brooks/Cole, Belmont, California, 1966, Chapter 2.
[14] Alger, R. S., and Capner, E. L., "Basic Relationships in Military Fires, Phases III, V, VI, and VII," DOD-AGFSRL-75-4, NSWC and Stanford Research Institute, May 1975.

ACKNOWLEDGMENT: Grants from the U.S. Naval Research Laboratory made possible the collaboration efforts in this research.

News and Meetings

This section of FIRE TECHNOLOGY is devoted to meeting announcements, appointments, and brief news items that may be of interest to our readers. Contributions should be sent to The Editor, FIRE TECHNOLOGY, c/o National Fire Protection Association, 470 Atlantic Ave., Boston, MA 02210.

Jet Fuel Safety Research

As part of its continuing effort to reduce the hazards of post-accident aircraft fires, the Aircraft and Airports Safety Division of the National Aviation Facilities Experimental Center has erected a wing spillage test facility that will be used to test modified jet aircraft fuels.

The initial test series will be carried out using Jet A kerosine blended with a small amount — 0.3 to 0.5 percent — of FM9 a fuel modifying additive developed by Imperial Chemical Industries, Inc. The purpose of the high molecular weight additive is to prevent the fuel from forming a fine, explosive, easily ignited mist when it is released from ruptured fuel tanks in an accident.

The Center's Systems Research and Development Service has been attacking the fuel misting problem for many years. Early work was done with gelled and emulsified fuels. When released from broken fuel tanks, the gelled and emulsified fuels held together very well. They did not form fine mists and turn into fireballs in the presence of ignition sources. Unfortunately, they would not flow easily through an aircraft's fuel system, and they had a short storage life.

The FAA, in cooperation with other government agencies, turned its attention to a number of antimisting additives that would reduce the mist-forming tendency of air-sheared fuels in accidents without significantly altering the fuel's flow characteristics inside fuel systems.

ICI offered evaluation quantities of FM9, a long chain organic polymer. In 1976 at the U.S. Naval Weapons Center, China Lake, California, tests of Jet A fuel containing small amounts of FM9 showed some promise of minimizing the post-crash fireball that frequently occurs in an impact survivable crash.

Results of the tests at China Lake, along with laboratory tests at NAFEC, were encouraging enough to warrant further testing on a larger scale. It was for this reason that NAFEC designed the wing spillage facility to simulate fuel spewing from a ruptured wing tank into a high-speed airstream such as might be encountered in a survivable crash landing.

Agency researchers plan to encourage U.S. chemical companies to supply additional additive candidates for evaluation in NAFEC's fuel spillage facility.

If the tests are successful, the agency plans to carry the program into full-scale